International Journal of
INTELLIGENT SYSTEMS AND APPLICATIONS IN ENGINEERING
ISSN:2147-6799 www.ijisae.org Original Research Paper

Gammadion based Local Binary Pattern with Shearlet coefficients for Palmprint Recognition

John Prakash Veigas*[1], Sharmila Kumari M.[2], Suchetha N. V.[3]

Submitted: 27/04/2023 **Revised**: 28/06/2023 **Accepted**: 09/07/2023

Abstract: Palmprints are stable and unique information used for biometric identification. This paper devises a novel texture-based feature extraction method inspired by the Gammadion structure that recognizes an individual based on Palmprint. The Region of Interest (ROI) extracted from the palm is initially normalized using the Histogram equalization technique. The ROI is converted into the frequency domain using Shearlet transformation to represent it in an illumination invariant form. Then the gammadion structure-based feature extraction method is used. It generates multiple feature maps fed to a simple Convolutional Neural Network(CNN). The proposed methodology is invariant with illumination and noise. Four publicly accessible standard Palmprint databases (CASIA, IITD, Tongji, and PolyU2) are used for extensive experimentation. The result is then compared with existing state-of-art techniques. The experimental analysis shows that the proposed methodology obtains the highest accuracy of 99.45% for the PolyU2 dataset, which is superior to some existing methods in the literature.

***Keywords*:** *Gammadion Binary Patterns, Shearlet transform, Palmprint recognition; Illumination invariant*

1. Introduction

Biometric recognition has attracted significant interest over the past two decades. Palmprint features are much more stable than other biometrics and have discriminative characteristics [1] including texture, principal line, geometrics, and more. Variations in environmental factors, such as illumination, noise, and change in orientation during image capture, make it difficult to acquire high-quality images in real-world situations [2]. A wide variety of Palmprint recognition techniques have been developed, including low-resolution [3][4][5], high-resolution [6], multispectral [7], and 3-D Palmprint recognition [8]. These techniques have proven to be good in recognition performance. High-resolution Palmprint images provide a high degree of similar features in detail, such as minutiae, density, orientation, principal lines, etc., which requires high pixel density for the images (more than 500 pixels per inch) [6]. Over the recent years, most of the research on Palmprint recognition has predominantly focused on low-resolution Palmprint recognition due to a lack of good quality image-capturing devices [9][10].

In most cases, Palmprint recognition consists of two steps of Palmprint feature representation and matching [11].

[1] *A J Institute of Engineering and Technology, Mangaluru-575006 affiliated to Visvesvaraya Technological University, Belagavi, INDIA ORCID ID : 0000-0002-9783-601X*
[2] *PA College of Engineering, Mangaluru-574153, affiliated to Visvesvaraya Technological University, Belagavi INDIA*
ORCID ID : 0000-0002-0707-0891
[3] *Sri Dharmasthala Manjunatheshwara Institute of Technology, Ujire-574240, affiliated to Visvesvaraya Technological University, Belagavi, INDIA,ORCID ID : 0000-0003-4796-8222*
** Corresponding Author Email: john.veigas@gmail.com*

Palmprint feature representation aims to exploit discriminative features to make Palmprint more separable. The second step, being is to build and design effective classifiers to distinguish the extracted features. Without any doubt, Palmprint feature representation significantly affects the performance of Palmprint recognition. However, extracting the discriminative features remains a demanding task in Palmprint recognition. Although Spatial domains are widely used for image representation, others consider using frequency domain to represent the image. The majority of image representation techniques exclusively compute features in the spatial domain. Local Binary Pattern (LBP) is an efficient texture descriptor that encodes local structures of the image by comparing each pixel to its adjacent neighborhood pixels [12]. It is highly robust to rotation [13][14] and changes in illumination and has a lower computing complexity. As a result, it is suitable for touchless Palmprint recognition. Many times, LBP's single-directional pixel approach frequently fails to capture multidirectional patterns. Hence, it is appropriate for touchless Palmprint recognition.

In the frequency domain approaches such as Discrete Cosine Transform (DCT) [15], Discrete Wavelet transform (DWT) [16] Curvelet Wavelet transform [17], Dual-tree [18], and so on are utilized for illumination normalization. Yet, these have their own limitations. Detection of curvilinear as well as point singularity structures in an image is challenging. In addition, DWT is not the best choice for sparse appropriation [19]. DWT only captures high-frequency features along three different directions in an image, i.e., horizontal, vertical, and diagonal. In contrast,

illumination normalization based on DCT removes low-frequency components by discretizing some of the DCT components in the input. It is difficult to predict the amount of DCT coefficients to be eliminated as it depends on the input image and its modality. The Curvelet and Contourlet transforms are not properly aligned with the continuum domain theory, hence generating various artifacts as a consequence. With its multidirectional approach, the geometric multi-scale Shearlet transform solves the aforementioned disadvantages, allowing us to construct sensitive sparse representations of image data while retaining anisotropic properties. We choose Shearlet over the wavelet and curvelet transforms due to several reasons. Wavelet representations are useful for approximating features at points or singularities. Wavelets are incapable of dealing with the discontinuities that are present on the edges of ground borders, hence not ideal when dealing with multivariate data. Although curvelets can provide better edge feedback than wavelets, they have been inconvenient to use. Some researchers subsequently suggested contourlets, but the method lacks a correct continuum theory. By taking the directional features into account, the Shearlet transform was developed to overcome the limitations of the wavelet transform. The affine system employs three additional parameters, which include scaling, shear, and translation, to record the orientation of edges more precisely. To capture the micro-level features, we introduce a Gammadion-based binary pattern feature extractor inspired by photoconductive antennas [20] [21] for Palmprint recognition.

The significant contribution of this work is as follows:

1. Proposed a novel Gammadion binary pattern in the frequency domain using Shearlet transform for Palmprint recognition.
2. Incorporated Adaptive histogram equalization with gamma correction for illumination normalization for enhancement of the input Palmprint.
3. Systematic analysis is performed by comparing the proposed approach with other state-of-art schemes viz LBP, LDP, HOL, CR-CompCode, PCA-Net, VGG-16, VGG-19, and Alexnet.

The remainder of the paper is as follows: Section 2 provides a brief literature review of Palmprint recognition. Section 3 demonstrates the proposed methodology. Section 4 presents a discussion on the implementation and results of the proposed approach with existing state-of-the-art approaches. Finally, section 5 presents the conclusion with future scope.

2. Literature Review

In the existing literature, Palmprint recognition can be mainly classified into five different categories that include line-based, texture-based, local direction coding-based, sub-space learning-based, and deep learning-based. (1) Line-based techniques capture the principal lines and local lines in the Palmprint image and use them as the dominant features for Palmprint recognition [22] [23]. To improve the recognition accuracy multi-biometric features extraction technique is adopted that combines the principal line features from both the left and right Palmprint images using the Gabor filter [24]. (2) Texture-based techniques are implemented by leveraging the prevalent features of the input image to perform Palmprint recognition. A comparative study made by [12] of the texture-based descriptors such as LBP, LDP, and BSIF, along with their variants, provides better recognition accuracy [25][26][27][28]. (3) Sub-space learning-based methods covert the Palmprint image from high dimensional vector space to low dimensional representation. PCA, ICA, LDA, and KFD, along with variants, are some of the prominent methods in this category[29] [30]. (4) Local direction encoding methods encode each pixel according to the dominant direction in which it was captured [31][32]. Competitive code and robust line orientation code compute the one dominant orientation for extracting the directional features. Chen et al. [33] transformed the double orientation pattern into hash code for faster recognition. (5) Deep learning-based techniques train the model using deep CNN for feature extraction in order to obtain higher recognition accuracy. For instance, Meraoumia Abdallah, et al.[4] proposed PCAnet based[34] deep learning method that provides a promising result. Genovese et al. [35] proposed Gabor-PCA approach tuning with filter. Further John Veigas et al. [36] presented Genetic Algorithm Based Gabor CNN for Palmprint Recognition. Moreover, many other deep learning approaches were proposed which provide higher recognition accuracies.

When the Palmprint image is captured in a local environment, pose deformation, illumination, and rotational variations degrade the recognition accuracy. For example, Naveena et al.[37] detected features from texture, and Fei et al. [38] proposed multi-curvature pattern. Whenever the images are captured in an open or unconstrained environment, due to deformation, illumination variation, and scale variation in the Palmprint image result in degradation of the recognition accuracy. Fie et al. suggested a recognition method using Low-rank representation combined with principal line distance, which provides better robustness to the noise for contactless Palmprint images. Kumar [39] presented a similar approach for contactless palmprint identification with a more precise deformation alignment. In these works, accurate region-of-interest image alignment is based on handcrafted alignments are crucial for enhancing matching accuracy. Zaho et al. [40] presented a deep learning framework termed deep discriminative representation (DDR), which is a generic framework that

utilizes limited Palmprint training data. To address the performance degradation due to single view, a multi-view discriminant Palmprint recognition with feature concatenation was proposed. This approach is prone to the overfitting problem. The literature uses least square regression and subspace learning techniques to represent multi-view features [41][42].

The issue of illumination variation is tackled by using Adaptive histogram equalization with gamma correction that dynamically determines the intensity transformation function as per the characteristics of the input Palmprint image. The following section provides a detailed description of the methodology followed in this research work.

3. Methodology

This section briefs about the methodology adapted and describes the underlying theory behind the methodology's purpose. These include the proposed block diagram for the methods adopted and the employed gammadion structure.

3.1. Image Pre-processing

After capturing the image from the input device, pre-processing is essential in constructing any biometric system. Initially, the ROI is extracted by making use of the Otsu thresholding and edge Kirsch edge detector methods mentioned in [36]. Then illumination normalization is performed using adaptive histogram Equalization to remove the noise and illumination variations [43].

3.2. Representation of Digital Shearlet Coefficient

Digital Shearlet Coefficient is a geometric multiresolution transform. In order to generate Shearlet Coefficient, apply Translation, shearing and dilation operations on mother function $\varphi \in L^2(R^2)$.

The dilation matrix is given by D_x

$$D_x = \begin{bmatrix} \sqrt{x} & 0 \\ 0 & 1/\sqrt{x} \end{bmatrix} \quad \forall\, x \in R^+ \quad (1)$$

The Shearing matrix is given by S_y

$$S_y = \begin{bmatrix} 1 & y \\ 0 & 1 \end{bmatrix} \quad \forall\, y \in R \quad (2)$$

For a given image I(M,N) with M rows and N columns with mother function $\varphi \in L^2(R^2)$ the Shearlet system can be represented as,

$$I \rightarrow ST_\varphi I(x, y, \rho) = \langle I, \varphi_{x,y,\rho} \rangle \quad (3)$$

Shearlet system be influenced by three major parameters that is 1) Dilation parameter (x) which estimates different resolution or scales 2) The shearing parameter (y), measures the orientation 3)Positional parameter (ρ) measures the location. Therefore, the transformation using Shearlet can be stated as,

$$ST_\varphi I(x, y, \rho) = \int_{-\infty}^{\infty} I(q)\, \varphi_{x,y}(\rho - q) dq = I * \varphi_{x,y}(\rho) \quad (4)$$

The continuous Shearlet model can be stated as,

$$ST\{\varphi\} = \left\{ \varphi_{x,y,\rho} = \sqrt[4]{x^3}\, \varphi S_y D_x(. - \rho)) \right\} \quad \forall\, x, y \in R, \rho \in R^2 \quad (5)$$

Equation (5) holds good when the function $\varphi \in L^2(R^2)$ satisfies the permissibility condition [19]. Now discretization equivalent can be obtained by mapping $R \rightarrow Z$ as

$$ST\{\varphi\} = \left\{ \varphi_{k,l,m} = \sqrt[4]{2^{3k}}\, \varphi\left(S_l D_{2^j} . - m\right) \right\} \quad \forall k \in Z, m \quad Z^2 \quad (6)$$

Here Z represents the digital grid. At this point equal usage of the digital and continuous domain should be given as shearing matrix S_l maps to Z^2 to itself.

For a given digital signal $f \in L^2(Z^2)$, the Digital Shearlet Transformation can be represented as,

$$DST_{k,l,m} = ST_{k,l,m} \forall\ k \in \{0, K-1\}\ and\ |l| < \left\lceil \sqrt{2^j} \right\rceil \quad (7)$$

Here K denotes maximum number of scale being represented.

3.3. Representation of Illumination invariance using Digit Shearlet Coefficient

As per the illumination-reflectance model [43], a digital image I (M, N) can be denoted as

$$I(M, N) = R(M, N) * L(M, N) \quad (8)$$

Here R (M, N) and L (M, N) represent the illumination and reflectance components of the given digital image. The R (M, N) characterizes the Palmprint properties such as principle lines, ridges, minutia, etc. The component L (M, N) represents how much light incident onto the Palmprint surface.

Applying logarithm

$$\log_{10}(I) = \log_{10}(R) + \log_{10}(L) \quad (9)$$

$$\log_{10} R = \log_{10}(I) - \log_{10}(L) = \log_{10}(I/L) = \log_{10}(I/I_{reconstruct})$$

$$\Rightarrow R = \frac{I}{I_{reconstruct}} \quad (10)$$

Equation (10) gives the required illumination invariant reflectance part of the given image I.

$$\xi(M, N) = \begin{cases} 1 & \forall\, |DST^{HF}_{j,k,m}(M, N)| > T_h \\ 0 & otherwise \end{cases} \quad (11)$$

The shrinkage value is given by,

$$T_h = \frac{\rho^2}{\rho_x^2} \quad (12)$$

Where $\sigma = \frac{median|DST_{j,k,m}^{HF}(M,N)|}{0.6745}$

The coefficients are restructured with ξ (M, N) to obtain high frequency denoised coefficients

$$DSTmod_{j,k,m}^{HF}(x,y) = DST_{j,k,m}^{HF}(M,N) \times \xi\,(M,N) \quad (13)$$

The image is the reconstructed using the $DSTmod_{j,k,m}^{HF}(M,\mathrm{N})$ bands and the unaltered bands $DST_{j,k,m}^{HF}(\mathrm{x},\mathrm{y})$

features on the neighborhood pixels using simple thresholding. A value of 1 is assigned to neighbors in a predefined patch with a grey level greater than the center pixel; otherwise, 0 is assigned. There are many extensions and alterations for the LBP method suggested, namely Boosted LBP, in which the Palmprint region is scanned with a scalable sub-window from which LBP histograms are extracted. Dominant LBP, Local LDP, Local Quaternary Pattern (LQP), Local Ternary Pattern (LTP), etc. [12]. Nevertheless, LBPs one-direction pixel difference technique frequently fails to record directional patterns in the Palmprint [45]. Inspired by these facts, this paper employs a multidirectional binary pattern motivated by the Gammadion structure [21].

The Gammadion structure with four different pixel

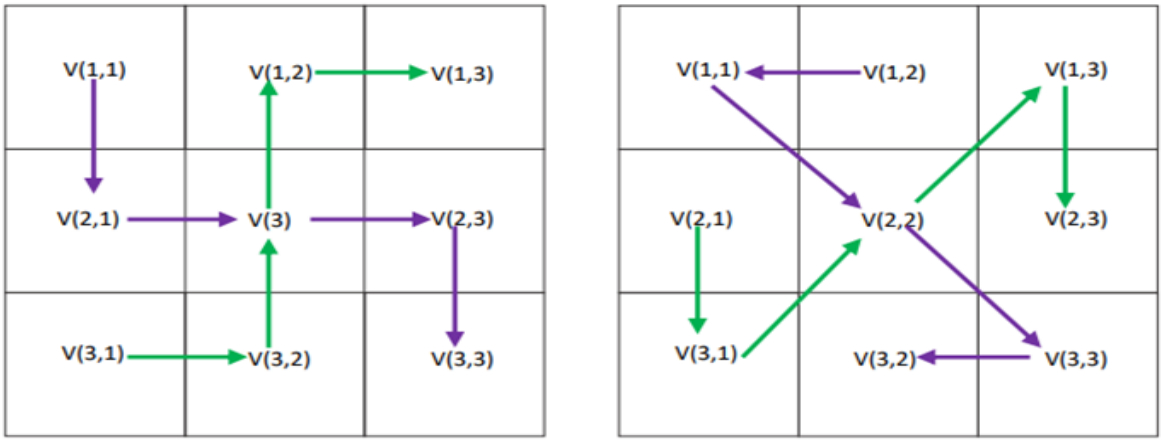

Fig.1. structure of Gammadion based binary pattern descriptor

$$I_{recons} = W^{-1}\left(DSTmod_{j,k,m}^{HF}(M,N), DST_{j,k,m}^{HF}(M,N)\right) \quad (14)$$

where, W_{DST}^{-1} represents the inverse Shearlet transformation operation. To approximation the component of reflectance R_{est},

I_{recons} should be replaced with $R_{est} = \frac{I}{I'_{recons}}$.

In addition, inspired by Lai et al. [44], incorporates the tangent inverse operation on R_{est} to further remove the noise effect in the invariant illumination feature map.

$$\sigma_y^2 = \frac{1}{PXQ}\sum_{x=1}^{p}\sum_{y=1}^{q} DST_{j,k,m}^{HF}(\mathrm{M},\mathrm{N})^2 \quad (15)$$

3.4. Gammadion binary pattern representation

Local pattern feature extraction approaches are becoming popular for extraction of patterns and to perform classification tasks in recent years. Local Binary Pattern (LBP) is the most prevalent method to tackle machine vision and pattern recognition problems among researchers [12]. LBP transforms the image into a binary pattern and extracts

sequence patterns is shown in the figure 1. The pattern can be generated using (16).

$$GBP_k = \sum_{k=1}^{4} \begin{matrix} f(V(j,k+1) - V(j,k))2^{k-1} \\ \forall\, j \in \{1,2\} \end{matrix} \quad (16)$$

$$f(p) = \begin{Bmatrix} 1 & p \geq 0 \\ 0 & otherwise \end{Bmatrix} \quad (17)$$

where, k denotes any of the GBP patterns as shown in Figure-1. Subsequently we obtain different directional binary patterns from a Palmprint image.

Sample Points:$\{V(1,1), V(1,2), V(1,3), V(1,4), V(1,5)\}$
GBP-1: 1 1 0 1 =13
Points:$\{V(2,1), V(2,2), V(2,3), V(2,4), V(2,5)\}$
GBP-2: 0 1 0 1=5
Points:$\{V(1,1), V(1,2), V(1,3), V(1,4), V(1,5)\}$
GBP-3: 0 1 0 1=5
Sample Points:$\{V(2,1), V(2,2), V(2,3), V(2,4), V(2,5)\}$
GBP-4: 0 1 0 1=5

3.5. Convolutional Neural Network(CNN)

CNN is an extensively researched and widely used area in the field of deep learning. It is a multilayer network model enriched from a backpropagation neural network algorithm. The CNN uses feed forward propagation to compute output values and backward propagation to compute the network weights and biases. In short, CNN repeatedly performs convolution and pooling on the enhanced input image to produce the classification.

Figure 2 shows the block diagram of the proposed approach. Initially, the ROI extracted from the Palmprint is normalized using Adaptive Histogram Equalization, then transformed into the frequency domain using Shearlet transform. The generated gammadion binary patterns are generated using (16). These patterns are fused using level 5 wavelet transform [46]. The fused images are trained using a simple CNN. The input query image is classified using the trained model during testing

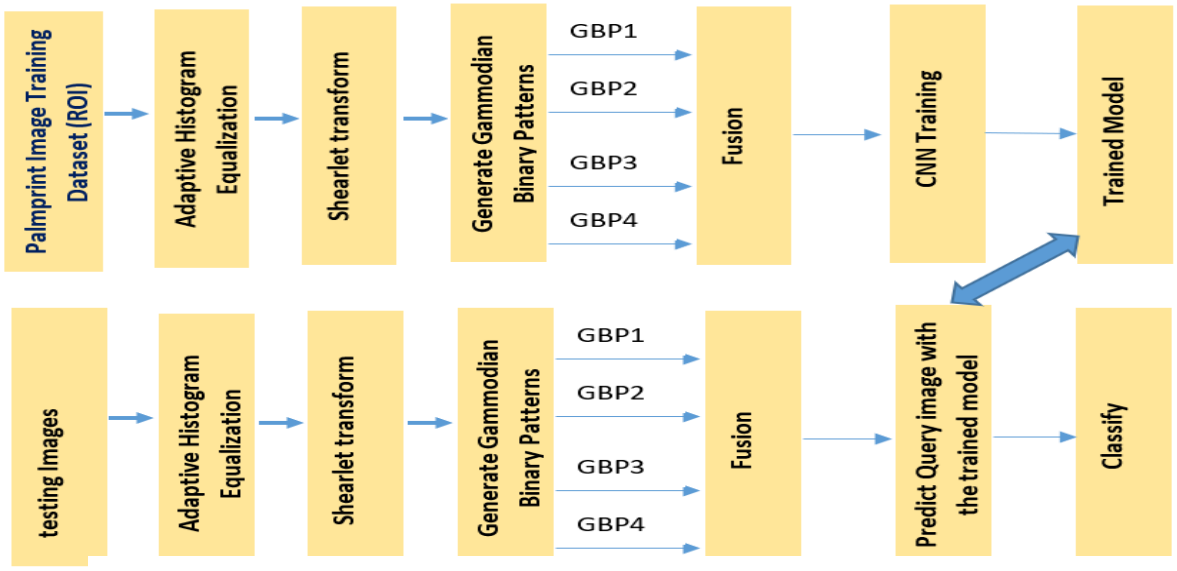

Fig.2. Block Diagram of the proposed approach

4. Implementation and results

This section details the implementation and outcomes obtained for the popular standard datasets. Experiments are carried out on Intel-Xeon(R) 2.30 GHz processors with NVIDIA Tesla K80 GPUs. Accuracy, EER, and Receiver Operating Characteristic Curves are used to evaluate the final results.

4.1. Datasets used

The presented methodology is assessed using four publicly accessible databases. Firstly, IIT Delhi Palmprint Database V1 is used, which was created by the Indian Institute of Technology Delhi and contained contactless Palmprint images from 230 individuals. Secondly, The CASIA Palmprint Database comprises 5502 Palmprints from 312 individuals.

Thirdly, the Tongji Palmprint consists of 600 Palmprint images belonging to 600 individuals. PolyU2 dataset has 7752 grayscale palmprint images belonging to 386 individuals.

4.2. Performance evaluation

To evaluate the performance of the Palmprint recognition system, various evaluation metrics such as accuracy, recall, precision, and F1 score are used to examine the model's reliability.

Accuracy is the fraction of Palmprint images correctly classified over the entire set of images. Equation (18) is used to compute the accuracy of the classification.

$$Accuracy = \frac{(TP+TN)}{S} \quad (18)$$

Where TP, TN and S are True Positive(TP), True Negative(TN) and Total number of images respectively.

Precision is the ratio of true positive to the sum of true positive and true negative is depicted in (19).

$$Precision = \frac{TP}{(TP+TN)} \quad (19)$$

Recall is the ratio of true positive and sum of false negative and true positives is denoted in (20)

$$Rec\,a\,ll = \frac{TP}{(TP+FN)} \quad (20)$$

Where TP, FN is true positives and false negatives respectively.

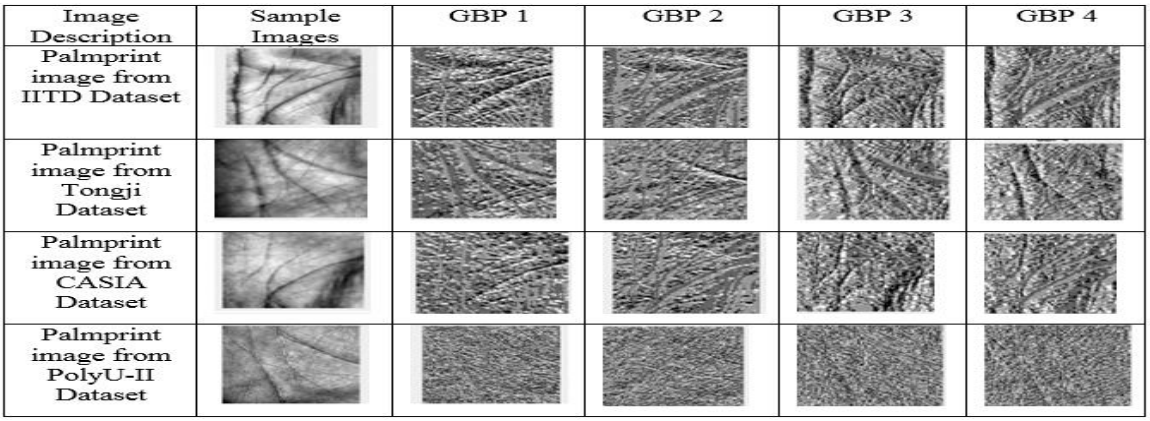

Fig.3. Gammadion Pattern generated for different dataset ROI images

The F1 score, which is shown in (21), is defined as the harmonic mean of precision and recall.

$$F1\ Score = \frac{2*(Precision* R\ ecall)}{(P\ recision + R\ ecall)} \qquad (21)$$

4.3. Experimentation:

Initially, the image from the dataset is converted to grayscale. The image background is removed, and the hand contour is pull out using the Otsu thresholding and edge Kirsch edge detector methods. From the hand contour, we extract the valley points corresponding to the index, middle and little finger by analyzing the local minima. ROI is extracted using the reference system based on the extracted valley points. 128*128 pixels ROI are extracted from the original dataset. Adaptive contrast limited adaptive histogram equalization and gamma correction [43] is applied to the ROI. The experiment is carried out using three variations. In the first type, the ROI is directly fed to CNN. We term it as 'raw pixels+CNN'. The second variation from the ROI gammadion binary pattern is obtained and fed to the CNN. We term this as 'GBP+CNN'. Figure 3 shows the Gammadion Pattern generated for different dataset ROI images. Finally, the Shearlet transform is applied to ROI in the third variation, and the

gammadion binary pattern is obtained which is termed as ‘GBPST+CNN. The patterns are fused and fed to a simple CNN. We discuss the results obtained in the next section by comparing them with other state-of-the-art techniques.

4.4 Results and Discussions

Table 1 shows the identification results of different methods such as LBP, LDP, HOL, CR-Comp Code, PCA-net, VGG-16, VGG-19, Alexnet with Raw Pixel + CNN,' GBP+CNN' and 'GBPST +CNN' on the IITD database. From the obtained results, one can see from Table 1 that the proposed 'GBPST +CNN attains the maximum identification percentage of accuracy, precision, recall, and F-1 Score of 98.42,0.97,0.97 and 0.96, respectively. The accuracy of Gammadion based binary pattern with Shearlet transformation with CNN is improved by 2.3% and 0.2% as compared to Alex net and PCA-Net respectively. It is also observed that the accuracy improvement is approximately 6% as compared to VGG-16 and VGG-19 models.

Table 1. Performance metrics for IITD Dataset

Sl no	Method	Precision	Recall	F-1 Score	accuracy (%)
1.	LBP	0.91	0.92	0.92	92.81
2.	LDP	0.82	0.83	0.83	85.17
3.	HOL	0.92	0.94	0.93	95.90
4.	CR-Comp Code	0.92	0.91	0.91	94.44
5.	PCA-Net	0.94	0.96	0.95	98.23
6.	VGG-16	0.92	0.89	0.91	92.56
7.	VGG-19	0.91	0.90	0.91	92.25
8.	Alexnet	0.96	0.94	0.95	96.1
9.	**Raw Pixels+ CNN**	**0.91**	**0.90**	**0.91**	**91.8**
10.	**GBP + CNN**	**0.94**	**0.93**	**0.94**	**94.3**
11.	**GBPST + CNN**	**0.96**	**0.97**	**0.97**	**98.42**

In contrast, GBP with CNN achieves an accuracy percentage, precision, and F-1 score of 94.3,0.94,0.93, and 0.94. The raw pixel with CNN achieves an accuracy percentage, precision, and F-1 score of 91.8,0.91,0.90, and 0.91. It is observed that the proposed methodology performs better as compared to other state-of-the-art techniques.

Table 2. Performance metrics for Tongji Dataset

Sl no	Method	Precision	Recall	F-1 Score	accuracy (%)
1.	LBP	0.96	0.97	0.97	98.2
2.	LDP	0.94	0.93	0.94	95.18
3.	HOL	0.97	0.95	0.96	98.3
4.	CR-Comp Code	0.95	0.96	0.95	98.82
5.	PCA-Net	0. 97	0.95	0.96	98.65
6.	VGG-16	0.93	0.92	0.93	94.28
7.	VGG-19	0.90	0.92	0.90	94.22
8.	Alexnet	0.92	0.93	0.92	98.88
9.	**Raw Pixels+ CNN**	**0.92**	**0.91**	**0.91**	**94.12**
10.	**GBP + CNN**	**0.94**	**0.95**	**0.95**	**96.53**
11.	**GBPST + CNN**	**0.98**	**0.94**	**0.96**	**99.22**

Table 2 shows the performance metric results of the proposed methodology for the Tonji palmprint dataset. The results clearly show that the proposed 'GBPST + CNN' has the highest performance metrics with an accuracy percentage, precision, Recall and F-1 score of 99.22,0.98,0.94 and 0.96, respectively. On the other hand, GBP+CNN performs short with an accuracy percentage, precision,Recall and F-1 score of 96.53,0.94, 0.95 and 0.95. The raw pixel with CNN achieves an accuracy percentage, precision, and F-1 score of 94.12,0.92,0.91, and 0.91. The proposed methodology outperforms the other state-of-the-art techniques listed in table.

Table 3 shows the performance metrics of the proposed approach for the PolyU-II dataset. It is apparent from the results that the GBPST+CNN method has an accuracy percentage, precision, recall, and F-1 score of 99.45,0.95,0.94 and 0.96. It is noted that GBP+CNN has an accuracy percentage, precision, recall, and F-1 score of 97.48,0.92,0.94 and 0.95. The raw pixel with CNN achieves an accuracy percentage, precision, and F-1 score of 95.83,0.90,0.93, and 0.92. It is apparent from the performance metrics that GBPST+CNN performs better than the other techniques, as listed in table 3.

Table 3. Performance metrics for PolyU-2 Dataset

Sl no	Method	Precision	Recall	F-1 Score	accuracy (%)
1.	LBP	0.95	0.96	0.94	98.9
2.	LDP	0.95	0.94	0.95	98.28
3.	HOL	0.94	0.96	0.95	98.21
4.	CR-Comp Code	0.96	0.97	0.97	98.11
5.	PCA-Net	0.95	0.96	0.96	98.78
6.	VGG-16	0.94	0.95	0.95	97.14
7.	VGG-19	0.93	0.94	0.94	96.04
8.	Alexnet	0.93	0.95	0.95	94.32
9.	**Raw Pixels+ CNN**	**0.90**	**0.93**	**0.92**	**95.83**
10.	**GBP + CNN**	**0.92**	**0.94**	**0.95**	**97.48**
11.	**GBPST + CNN**	**0.95**	**0.94**	**0.96**	**99.45**

Table 4 lists the performance measures obtained for the proposed technique with the CASIA Palmprint dataset. It is observed that GBPSC+CNN has a maximum identification performance with accuracy percentage, precision, recall, and F-1 score of 98.17,0.98,0.94.96, respectively. It is noted that GBP+CNN has an accuracy percentage, precision, recall, and F-1 score of 96.85,0.94.0.97 and 0.96.

Table 4. Performance metrics for CASIA Dataset

Sl no	Method	Precision	Recall	F-1 Score	accuracy (%)
1.	LBP	0.94	0.96	0.95	97.3
2.	LDP	0.91	0.93	0.92	97.91
3.	HOL	0.94	0.95	0.95	97.96
4.	CR-Comp Code	0.94	0.92	0.93	96.33
5.	PCA-Net	0.96	0.93	0.95	98.37
6.	VGG-16	0.91	0.89	0.90	92.14
7.	VGG-19	0.92	0.92	0.92	92.16

8.	Alexnet	0.91	0.92	0.92	92.73
9.	**Raw Pixels+ CNN**	**0.92**	**0.93**	**0.93**	**93.64**
10.	**GBP + CNN**	**0.94**	**0.97**	**0.96**	**96.85**
11.	**GBPST + CNN**	**0.98**	**0.94**	**0.96**	**98.17**

The raw pixel with CNN achieves an accuracy percentage, precision, and F-1 score of 93.64,0.92,0.93, and 0.93 It can be seen that GBPST+CNN produces better results than the other state-of-the-art techniques listed in table 4.The overall improvement in accuracy of proposed '**GBPST + CNN'** in the case of CASIA dataset is 5.13% and 0.67% respectively as compared to the Alex-net and PCA-net respectively. Further it is observed clearly that proposed methodology outperformces the state of art technqies such as LBP, LDP, HOL, CR-CompCode, PCA-net, VGG-16,VGG-19 and Alexnet.

5. Conclusion and future work

We have proposed a texture-based approach for Palmprint recognition. In this approach, a Gammadion Binary Pattern of Shearlet coefficients are proposed and implemented. It is suitable for high or low-resolution Palmprint images. Experimental results show that the proposed approach yields better classification accuracy and has relatively high robustness to the variations of orientation, position, and illumination. Extensive experimentation is carried out on four publicly available standard Palmprint databases. Comprehensive experiments have been undertaken to evaluate the system's performance, and the test results confirm the efficacy of the proposed technique, which can produce a good result. In the future, the Gabor filter instead of Shearlet can be used and compared to find the efficiency of the methods.

Author contributions

John Prakash Veigas: Conceptualization, Methodology, training and validation, writing original draft preparation and editing **Sharmila Kumari M:** Data curation, writing review and editing, supervision, Validation **Suchetha N V:** Reviewing and Editing and proofreading.

Conflicts of interest

The authors declare no conflicts of interest.

References

[1] N. Duta, A. K. Jain, and K. V. Mardia, "Matching of palmprints," *Pattern Recognit. Lett.*, vol. 23, no. 4, pp. 477–485, Feb. 2002.

[2] A. Morales, M. A. Ferrer, and A. Kumar, "Towards contactless palmprint authentication," *IET Comput. Vis.*, vol. 5, no. 6, pp. 407–416, 2011.

[3] D. Zhang, W. K. Kong, J. You, and M. Wong, "Online palmprint identification," *IEEE Trans. Pattern Anal. Mach. Intell.*, vol. 25, no. 9, pp. 1041–1050, 2003.

[4] and A. B. Abdallah Meraoumia, Farid Kadri, Hakim Bendjenna, Salim Chitroub, "Improving Biometric Identification Performance Using PCANet Deep Learning and Multispectral Palmprint," *Biometric Secur. Priv.*, pp. 51–69, 2017.

[5] X. Wang, L. Lei, and M. Wang, "Palmprint verification based on 2D - Gabor wavelet and pulse-coupled neural network," *Knowledge-Based Syst.*, vol. 27, pp. 451–455, 2012.

[6] J. Dai, J. Zhou, and S. Member, "Multifeature-Based High-Resolution Palmprint Recognition," vol. 33, no. 5, pp. 945–957, 2011.

[7] J. Grover and M. Hanmandlu, "The fusion of multispectral palmprints using the information set based features and classifier," *Eng. Appl. Artif. Intell.*, vol. 67, pp. 111–125, Jan. 2018.

[8] S. Trabelsi, D. Samai, F. Dornaika, A. Benlamoudi, K. Bensid, and A. Taleb-Ahmed, "Efficient palmprint biometric identification systems using deep learning and feature selection methods," *Neural Comput. Appl.*, vol. 4, 2022.

[9] L. Fei, G. Lu, W. Jia, S. Teng, and D. Zhang, "Feature extraction methods for palmprint recognition: A survey and evaluation," *IEEE Trans. Syst. Man, Cybern. Syst.*, vol. 49, no. 2, pp. 346–363, Feb. 2019.

[10] A. S. Tarawneh, D. Chetverikov, and A. B. Hassanat, "Pilot Comparative Study of Different Deep Features for Palmprint Identification in Low-Quality Images," *Ninth Hungarian Conf. Comput. Graph. Geom.*, pp. 3–8, 2018.

[11] D. Zhong, X. Du, and K. Zhong, "Decade progress of palmprint recognition: A brief survey," *Neurocomputing*, vol. 328, pp. 16–28, 2019.

[12] A. El Idrissi, Y. El Merabet, and Y. Ruichek, "Palmprint recognition using state-of-the-art local texture descriptors: A comparative study," *IET Biometrics*, vol. 9, no. 4, pp. 143–153, 2020.

[13] T. Ojala, M. Pietikäinen, and T. Mäenpää, "Multiresolution gray-scale and rotation invariant texture classification with local binary patterns," *IEEE Trans. Pattern Anal. Mach. Intell.*, vol. 24, no. 7, pp. 971–987, 2002.

[14] X. Wang, H. Gong, H. Zhang, B. Li, and Z. Zhuang, "Palmprint identification using boosting local binary pattern," *Proc. - Int. Conf. Pattern Recognit.*, vol. 3, pp. 503–506, 2006.

[15] X. Y. Jing and D. Zhang, "A face and palmprint recognition approach based on discriminant DCT feature extraction," *IEEE Trans. Syst. Man, Cybern. Part B Cybern.*, vol. 34, no. 6, pp. 2405–2415, 2004.

[16] L. Zhang and D. Zhang, "Characterization of Palmprints by Wavelet Signatures via Directional Context Modeling," vol. 34, no. 3, pp. 1335–1347, 2004.

[17] F. Liu, L. Zhou, Z. M. Lu, and T. Nie, "Palmprint feature extraction based on curvelet transform," *J. Inf. Hiding Multimed. Signal Process.*, vol. 6, no. 1, pp. 131–139, 2015.

[18] Y. Wang and Q. Ruan, "Dual-tree complex wavelet transform based local binary pattern weighted histogram method for palmprint recognition," *Comput. Informatics*, vol. 28, no. 3, pp. 299–318, 2009.

[19] G. Kutyniok, W.-Q. Lim, and X. Zhuang, "Digital Shearlet Transform," pp. 1–39, 2011.

[20] H. Suo *et al.*, "Polarization property of terahertz wave emission from gammadion-type photoconductive antennas," *Appl. Phys. Lett.*, vol. 103, no. 11, 2013.

[21] S. Koley, H. Roy, and D. Bhattacharjee, "Gammadion binary pattern of Shearlet coefficients (GBPSC): An illumination-invariant heterogeneous face descriptor," *Pattern Recognit. Lett.*, vol. 145, pp. 30–36, 2021.

[22] D. S. Huang, W. Jia, and D. Zhang, "Palmprint verification based on principal lines," *Pattern Recognit.*, vol. 41, no. 4, pp. 1316–1328, 2008.

[23] X. Wu, D. Zhang, K. Wang, and B. Huang, "Palmprint classification using principal lines," *Pattern Recognit.*, vol. 37, no. 10, pp. 1987–1998, Oct. 2004.

[24] Y. Xu, L. Fei, and D. Zhang, "Combining left and right palmprint images for more accurate personal identification," *IEEE Trans. Image Process.*, vol. 24, no. 2, pp. 549–559, 2015.

[25] S. Liao, M. W. K. Law, and A. C. S. Chung, "Dominant local binary patterns for texture classification," *IEEE Trans. Image Process.*, vol. 18, no. 5, pp. 1107–1118, 2009.

[26] Y. T. Luo *et al.*, "Local line directional pattern for palmprint recognition," *Pattern Recognit.*, vol. 50, pp. 26–44, 2016.

[27] S. Ma, Q. Hu, S. Zhao, W. Wu, and J. Wu, "Multi-Scale Multi-Direction Binary Pattern Learning for Discriminant Palmprint Identification," *IEEE Trans. Instrum. Meas.*, vol. 72, 2023.

[28] L. Fei, B. Zhang, Y. Xu, D. Huang, W. Jia, and J. Wen, "Local Discriminant Direction Binary Pattern for Palmprint Representation and Recognition," *IEEE Trans. Circuits Syst. Video Technol.*, vol. PP, no. c, p. 1, 2019.

[29] Tee, Connie and Ngo, David Chek Ling and Goh, Michael Kah Ong and Teoh, Andrew Beng Jin (2003) Palmprint Recognition with PCA and ICA. Conference of Image and Vision Computing New Zealand 2003 (IVCNZ'03). pp. 227-232.

[30] S. Zhao and B. Zhang, "Learning Salient and Discriminative Descriptor for Palmprint Feature Extraction and Identification," *IEEE Trans. Neural Networks Learn. Syst.*, vol. 31, no. 12, pp. 5219–5230, 2020.

[31] Z. Sun, T. Tan, Y. Wang, and S. Z. Li, "Ordinal palmprint represention for personal identification," in *Proceedings - 2005 IEEE Computer Society Conference on Computer Vision and Pattern Recognition, CVPR 2005*, 2005, vol. I.

[32] Z. Sun, L. Wang, and T. Tan, "Ordinal Feature Selection for Iris and Palmprint Recognition," *3922 IEEE Trans. IMAGE Process. VOL. 23, NO. 9, Sept. 2014*, vol. 23, no. 9, pp. 3922–3934, 2014.

[33] L. Fei, Y. Xu, W. Tang, and D. Zhang, "Double-orientation code and nonlinear matching scheme for palmprint recognition," *Pattern Recognit.*, vol. 49, pp. 89–101, 2016.

[34] K. Krajnak, S. Waugh, R. Miller, S. Li, and M. L. Kashon, "PCANet: A Simple Deep Learning Baseline for Image Classification?," *40th Int. Congr. Expo. Noise Control Eng. 2011, INTER-NOISE 2011*, vol. 4, no. 12, pp. 3552–3556, 2011.

[35] A. Genovese, V. Piuri, K. N. Plataniotis, and F. Scotti, "PalmNet: Gabor-PCA convolutional networks for touchless palmprint recognition," *IEEE Trans. Inf. Forensics Secur.*, vol. 14, no. 12, pp. 3160–3174, Dec. 2019.

[36] J. P. Veigas, M. S. Kumari, and G. S. Satapathi, "Genetic Algorithm Based Gabor CNN For Palmprint Recognition," *Int. J. Recent Technol. Eng.*, vol. 8, no. 6, pp. 4895–4899, 2020.

[37] C. Naveena, S. Rangappa, and Chethan H. K., "Texture Features in Palmprint Recognition System," *Int. J. Nat. Comput. Res.*, vol. 10, no. 1, pp. 41–57, Jan. 2021.

[38] L. Fei, B. Zhang, S. Teng, Z. Guo, S. Li, and W. Jia, "Joint Multiview Feature Learning for Hand-Print Recognition," *IEEE Trans. Instrum. Meas.*, vol. 69, no.

12, pp. 9743–9755, Dec. 2020.

[39] A. Kumar, "Toward More Accurate Matching of Contactless Palmprint Images under Less Constrained Environments," *IEEE Trans. Inf. Forensics Secur.*, vol. 14, no. 1, pp. 34–47, 2019.

[40] S. Zhao and B. Zhang, "Deep discriminative representation for generic palmprint recognition," *Pattern Recognit.*, vol. 98, Feb. 2020.

[41] T. Shu, B. Zhang, and Y. Y. Tang, "Multi-View Classification via a Fast and Effective Multi-View Nearest-Subspace Classifier," *IEEE Access*, vol. 7, pp. 49669–49679, 2019.

[42] S. Zhao, J. Wu, B. Zhang, and L. Fei, "Low-rank inter-class sparsity based semi-flexible target least squares regression for feature representation," *Pattern Recognit.*, vol. 123, Mar. 2022.

[43] S. C. Huang, F. C. Cheng, and Y. S. Chiu, "Efficient contrast enhancement using adaptive gamma correction with weighting distribution," *IEEE Trans. Image Process.*, vol. 22, no. 3, pp. 1032–1041, 2013.

[44] Y. F. Yu, D. Q. Dai, C. X. Ren, and K. K. Huang, "Discriminative multi-layer illumination-robust feature extraction for face recognition," *Pattern Recognit.*, vol. 67, no. 6, pp. 201–212, 2017.

[45] L. Liu, L. Zhao, Y. Long, G. Kuang, and P. Fieguth, "Extended local binary patterns for texture classification," *Image Vis. Comput.*, vol. 30, no. 2, pp. 86–99, Feb. 2012.

[46] H.Li, B.S. Manjunath, and S.K. Mitra, "Multisensor Image Fusion Using the Wavelet Transform," *Graphical Models and Image Processing*, vol. 57, no. 3. pp. 235–245, 1995.

[47] Tamilselvi, T. ., Lakshmi, D. ., Lavanya, R. ., & Revathi, K. . (2023). Digital Companion for Elders in Tracking Health and Intelligent Recommendation Support using Deep Learning. International Journal on Recent and Innovation Trends in Computing and Communication, 11(3), 145–152. https://doi.org/10.17762/ijritcc.v11i3.6331

[48] Maria Gonzalez, Machine Learning for Anomaly Detection in Network Security , Machine Learning Applications Conference Proceedings, Vol 1 2021.